Combining small-molecule bioconjugation and hydrogen-deuterium exchange mass spectrometry (HDX-MS) to expose allostery: the case of human cytochrome P450 3A4

Julie Ducharme, Vanja Polic, Christopher J. Thibodeaux*, Karine Auclair*

Department of Chemistry
McGill University
801 Sherbrooke Street West, Montréal, Québec, Canada H3A 0B8
k.auclair@mcgill.ca

Abstract: We report a novel approach to study allostery which combines the use of carefully selected bioconjugates and hydrogen-deuterium exchange mass spectrometry (HDX-MS). This strategy avoids issues related to weak substrate binding and ligand relocalization. The utility of our method is demonstrated using human cytochrome P450 3A4 (CYP3A4), the most important drug-metabolizing enzyme. Allosteric activation and inhibition of CYP3A4 by pharmaceuticals is an important mechanism of drug interactions. We performed HDX-MS analysis on several CYP3A4-effector bioconjugates, some of which mimic the allosteric effect of positive effectors, while others show activity enhancement even though the label does not occupy the allosteric pocket (agonistic), or do not show activation while still blocking the allosteric site (antagonistic). This allowed us to better define the position of the allosteric site, the protein structural dynamics associated with allosteric activation, and the presence of co-existing conformers.

Introduction

Allosteric regulation is essential to metabolism and cell signaling, thereby offering an important source of new drug targets.[1–5] It is a ubiquitous phenomenon by which structural information is propagated spatially between distinct sites across the structure of macromolecular systems. Typically, an effector binds to an allosteric site, and this binding event modulates the functional activity at a remote site by triggering a reorganization of protein intramolecular interactions. Despite its central role in biology, however, the molecular basis of allostery remains largely uncharacterized in most enzymes,[6,7] hampering our ability to fully understand the biophysical mechanisms underlying both life and disease.

Human cytochrome P450 enzymes (CYPs) are heme monooxygenases that frequently exhibit atypical cooperative and allosteric behaviors.[8–10] CYP3A4 has attracted considerable interest for its contribution to the metabolism of approximately 50% of all clinical drugs[11] and for its involvement in adverse drug interactions and drug resistance. The exceptionally broad substrate specificity of CYP3A4 is a result of its active site plasticity, which can even accommodate multiple ligands simultaneously.[10,12] The kinetic behavior of CYP3A4 is further complicated by ligand binding at allosteric site(s).[13] Whereas the allosteric modulation of CYP3A4 has been kinetically defined for several effectors,[14–16] the structural mechanisms involved have not. These mechanisms are challenging to characterize given the large number of possible enzyme-ligand(s) complexes and the possibility that ligands may relocalize after initial binding.[17] Furthermore, most known effectors of CYP3A4 also compete with other substrates for oxidation.[17] Importantly, the location of the allosteric site remains a matter of debate. It may overlap with the active site (Figure S20) and even be dependent on the nature of the effector.[18,19] All of these characteristics make deconvolution of the different ligand binding events, as well as the relationship of these events to allosteric activation and catalytic activity particularly challenging to investigate.

Hydrogen-deuterium exchange mass spectrometry (HDX-MS) is a powerful approach for characterizing protein conformational flexibility. This technique probes reorganization in the hydrogen-bond network of secondary structural elements by monitoring the time-dependent exchange of deuterium atoms between the solvent and the amide moieties of the protein backbone.[20] The ability of CYP3A4 to bind multiple ligands concurrently and the possible relocalization of ligands in the enzyme may lead to heterogeneity in the system, thereby complicating HDX-MS data analysis and interpretation. Moreover, neither HDX-MS nor other methods used to study allostery discriminate between dynamic changes implicated in ligand binding from those involved in rate enhancement. To overcome these intrinsic limitations, we report herein a novel approach that combines bioconjugation and HDX-MS. Covalently attaching the effector greatly reduces sample heterogeneity and noise, thereby enhancing our ability to capture the structural dynamics changes specifically involved in enzyme activation.

Progesterone is a well-studied substrate and positive effector of CYP3A4. To probe the progesterone allosteric site and its impact on CYP3A4 catalysis, we previously developed a bioconjugation methodology to covalently attach a maleimide-progesterone (PGM) moiety near or at the allosteric site selectively.[21] This was used to identify allostery-mimicking, allostery-agonist and allostery-antagonist bioconjugates based on analysis of the catalytic activity and of enzyme activation by free progesterone.[22] After reaction with PGM, some bioconjugates (*e.g.* F108C-PGM, F215C-PGM and L482C-PGM) were found to display a large rate enhancement towards 7-benzyloxy-4-trifluoromethylcoumarin (BFC) oxidation, whereas others did not (*e.g.* G481C-PGM and bioconjugation of methyl-maleimide to F215C or F108C).[21,22] The enzyme activity was also measured in the presence of the positive effector progesterone.[22] As expected, the unconjugated F108C, F215C, G481C and L482C mutants were all stimulated by free progesterone, implying an intact allosteric pocket. In contrast, activation by free progesterone was abolished for F108C-PGM and F215C-PGM, suggesting that the allosteric pocket is occupied by the PGM moiety.[22] Together the enhanced activity and lack of activation by free progesterone observed for these two bioconjugates are consistent with an allostery-mimicking behavior.[22] In contrast, although PGM bioconjugation was also found to activate the L482C mutant, the addition of free progesterone to L482C-PGM resulted in further enhancement of activity, implying that the allosteric pocket was available, as expected for an agonist-like bioconjugate. Finally, although PGM bioconjugation did not significantly increase the activity of the G481C mutant, free progesterone had no effect on the activity of the G481C-PGM bioconjugate, indicating that the PGM-label is blocking access to the activator without triggering activation itself (an antagonistic behavior).

Herein we exploit these allostery-mimicking (F108C-PGM, F215C-PGM), agonist-like (L482C-PGM) and antagonistic (G481C-PGM) bioconjugates to further study allostery in CYP3A4.[22] We reasoned that this collection of CYP3A4-PGM bioconjugates would enable a robust HDX-MS characterization of allosteric mechanisms in CYP3A4. The results presented herein reveal that the structural dynamics of CYP3A4 are significantly affected by the location of the covalently-tethered PGM ligand. Importantly, comparison of the HDX-MS data for all four CYP3A4 mutants before and after PGM bioconjugation, allowed us to not only confirm the location of the allosteric site, but also to identify critical CYP3A4 structural elements involved in allosteric activation, thereby demonstrating the utility of our approach.

Results

Description of the HDX-MS workflow
Our study employs a typical continuous-labeling, bottom-up HDX-MS approach (Table S1). HDX was achieved by incubating enzymes in a buffered D_2O solution (pD = 7.0, >98% deuterium) for different periods of time (0.5-240 min). During this continuous exchange, the amide moieties of the protein backbone acquire solvent deuteria at a rate that is highly sensitive to the local hydrogen bonding environment of each amide.[23] Ligand binding (or PGM conjugation) can induce local and/or global fluctuations in the conformation of the protein, which may alter hydrogen bonding networks and, consequently, the rate of deuterium uptake at a given amide. Relative decreases in deuterium exchange typically reflect a structural organization or an intermolecular interaction with a ligand,

whereas relative increases in deuterium exchange suggest enhanced flexibility of the protein backbone.

The extent of deuterium uptake for wild type CYP3A4 after 240 min of H/D exchange is shown in Figure S3A. Our workflow resulted in a total of 77 unique, reproducibly-detected peptic peptides spanning 88% of the CYP3A4 amino acid sequence. Overlapping peptides were identified across most of the protein sequence, providing further validation for the uptake data. The deuterium uptake for each peptide over time can be visualized in Figure S3B, where the relative fractional deuterium uptake is plotted along the protein sequence. These data reveal that the N-terminus region of CYP3A4 is generally more structured than the C-terminus, with the most rigid regions located on the proximal side and in the direct vicinity of the heme, encompassing the *N*-terminus region, the A-, C-, J-, K- and L-helices, and most of the active site residues. Interestingly, the most flexible regions (Figure S3C, colored in red) are located mostly at positions distal to the heme group, and include the B/C-loop, part of the D-helix, and the F-G region, as well as the J'-helix of the proximal side. Consistent with our results, these regions were previously identified by Ekroos *et al.* as showing the highest variation in Cα RSMD based on alignment of the available crystal structures of CYP3A4.[24] In their recent HDX-MS study of CYP3A4 in lipid nanodiscs, Treuheit *et al.* also identified the F-G region, B/C-loop and C-terminus as the most flexible areas of the enzyme.[25] Finally, using double electron-electron resonance (DEER), Cho *et al.* reported significant ligand-dependent changes in the motion of the F/G region of a soluble, truncated CYP3A4 variant.[26]

The aggregation of CYP3A4 in solution is a well-known phenomenon.[27] In order to verify if CYP3A4 aggregation was causing any perturbation in the HDX measurements that would potentially bias the data interpretation, we measured deuterium uptake by CYP3A4 over a range of enzyme concentrations (0.5, 1, 2, 5 μM). We observed no significant deuterium uptake differences (CI 98%) in any of the detected peptides (Figure S14), suggesting that artifactual CYP3A4 aggregation is not significantly contributing to the quantitation of deuterium uptake in our study.

HDX profiles of CYP3A4-PGM conjugates highlight regions involved in allosteric activation
To determine how PGM bioconjugation affects protein conformation, HDX profiles were compared before and after PGM-bioconjugation (differential HDX) for the F108C and F215C mutants of CYP3A4. These bioconjugates have been previously shown to mimic progesterone allosteric activation.[22] The relative fractional uptake (RFU) differences between the free F108C and F215C enzymes and their PGM-bioconjugates are shown in Figure 1. In this representation of the HDX data, regions of the protein shaded blue and red undergo less and more deuterium exchange, respectively, in the presence of the conjugated PGM moiety. The RFU differences measured in triplicate at each exchange time point were summed together, enabling us to capture more subtle changes in HDX with higher statistical confidence (all HDX difference data in this study are reported at the 98% confidence interval).[28] Several regions of the F108C and F215C mutant enzymes exhibited similar changes in deuterium uptake upon PGM conjugation (Figure 2A). We reasoned that these regions are likely to report on allosteric signaling networks shared by both the F108C and F215C enzymes. Namely, the first portion of the E-helix, the F´-helix, the G´-helix, the K/β1-loop, and the β1-sheet all undergo rigidification in both enzymes upon PGM labeling, whereas the F-helix becomes more flexible.
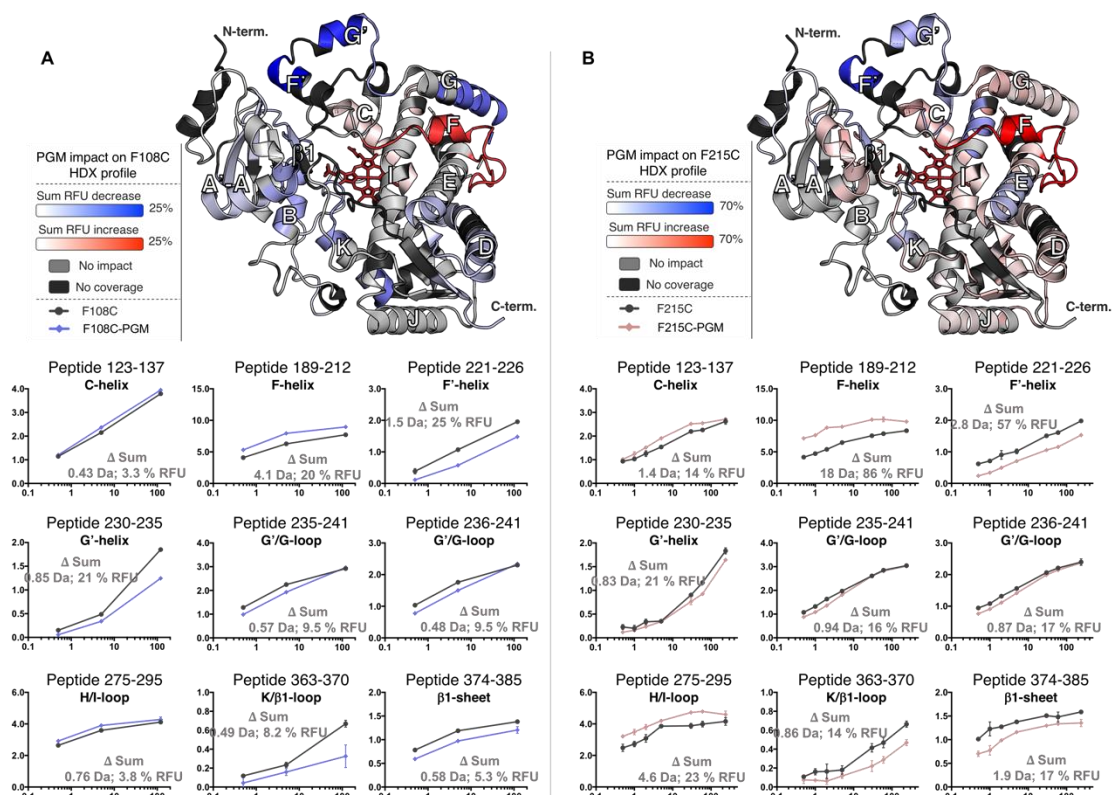
Figure 1. Differential HDX profiles of the allostery-mimicking PGM-bioconjugates. The significant (CI 98%) sum of the relative fractional uptake differences (RFU) are mapped on the CYP3A4 structure for the F108C (**A**) and F215C (**B**) mutants upon PGM bioconjugation (PDB: 1W0F). The total sum comprised three time points for the F108C mutant (0.5, 5, 120 min) and seven time points for the F215C mutant (0.5, 1, 2, 5, 30, 60, 240 min). The red and blue colors indicate protein segments that exchange more and less deuterium, respectively, with PGM conjugation. The light gray regions did not undergo a significant change in uptake upon PGM bioconjugation and the black regions were not covered in the mass spectrometry analysis. For each enzyme, deuterium uptake plots are shown for the nine common peptides that underwent the largest change in RFU (summed over all time points) following PGM conjugation. The total summed D uptake and RFU difference value is indicated on each graph. The complete list of peptides that underwent significant H/D exchange with PGM conjugation is provided in Figure S5 (coverage maps), S8 and S9 (D uptake plots).

The rigidification of peptides in the F´-G´-helices, which comprise a portion of the previously proposed allosteric binding site,[29,30] are consistent with binding of the PGM label at this location in both bioconjugates. Although largely similar, the differential HDX profiles for these two mutants do show some minor differences, such as in the A'-A-helices, the G-helix and D/E-loop which become more rigid in the F108C-PGM conjugate and more flexible in the F215C-PGM conjugate. These minor disparities may be attributed to the different covalent PGM attachment sites, which may have a small effect on the PGM binding orientation in the allosteric pocket.
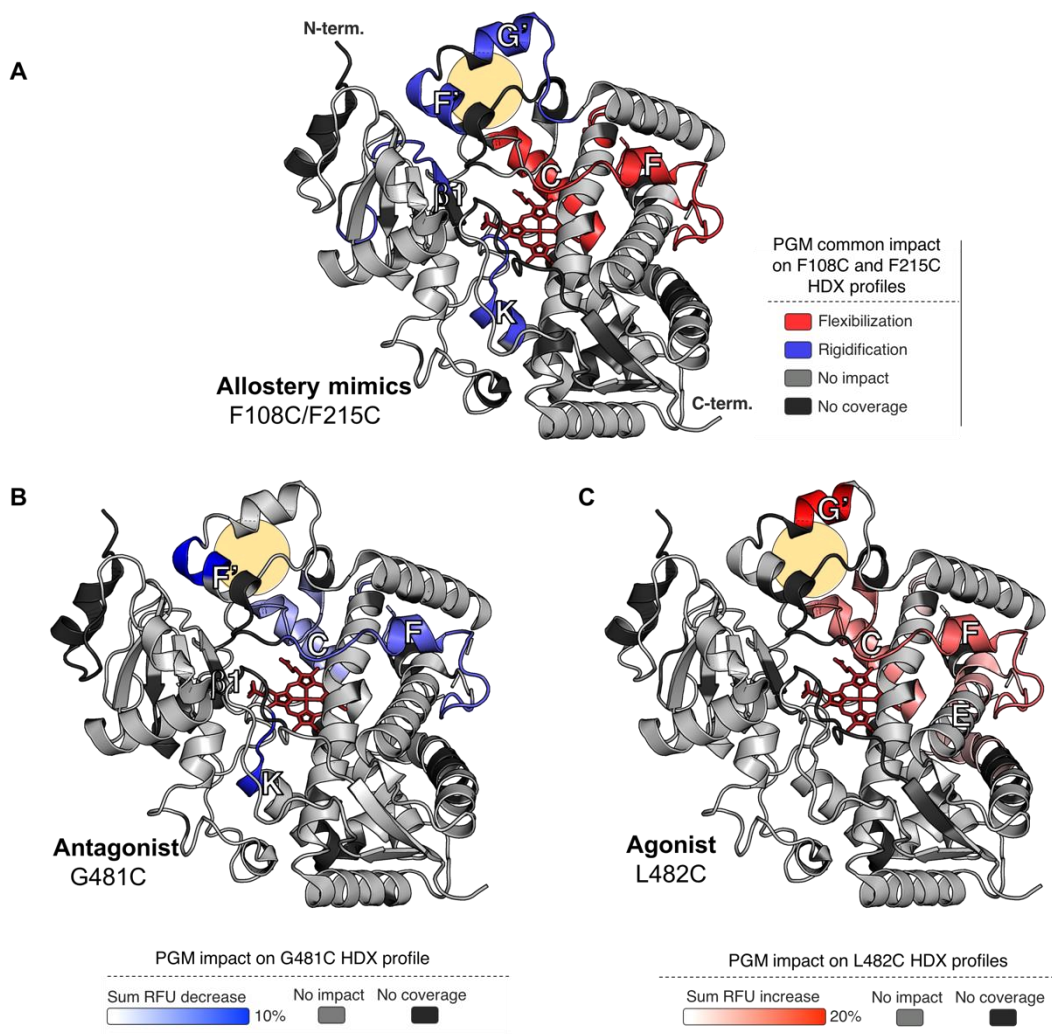
Figure 2. Differential HDX profiles of the allostery mimics (F108C, F215C) (**A**), the antagonist (G481C) (**B**), and the agonist (L482C) (**C**) PGM-conjugates. Regions highlighted in blue are becoming more rigid after PGM bioconjugation, whereas regions in red are becoming more flexible. A yellow circle designates the approximate position of the putative allosteric site of CYP3A4. The light gray regions did not undergo a significant change in uptake upon PGM bioconjugation and the black regions were not covered in the mass spectrometry analysis. In (**A**) the common changes in deuterium uptake for both allostery mimics are combined. In (**B**) and (**C**), the total significant (CI 98%) sum of the relative fractional uptake differences (RFU) are mapped on the CYP3A4 structure (PDB: 1W0F). The total sum is comprised of two time points (5, 60 min) for both mutants. The complete list of peptides that underwent significant H/D exchange upon PGM conjugation is provided in Figure S6 (coverage maps), S10 and S11 (D uptake plots).

Finally, recognizing that substrate binding to the active site may also affect the HDX properties of CYP3A4, we obtained the HDX-MS profile of F215C-PGM in the presence of 100 mM testosterone, a well-studied CYP3A4 substrate (Figure S4, S7, S13). A few minor differences were observed when compared to the HDX profile of F215C-PGM. Testosterone binding decreased the flexibilization of the C-helix induced by PGM-labeling and increased the flexibility of the F-helix region. The A'-A helices and β4-sheet were also more rigid in presence of the testosterone substrate. All of the other dynamics perturbations observed in the F215C-PGM state were preserved (e.g., rigidification of the F'-helix and the K/b1-loop, flexibilization of the H/I-loop). These

studies demonstrate the potential of our bioconjugation approach for deconvoluting structural perturbations induced by ligand binding to the allosteric and active sites.

Differential HDX of the antagonistic and agonistic PGM-conjugates define functionally relevant structural dynamics changes

To further confirm the conclusions reached using the allostery-mimicking PGM-conjugates, we next compared the HDX difference profiles of these enzymes with those of the antagonistic (G481C-PGM) and agonistic (L482C-PGM) bioconjugates. In the antagonistic system, the PGM moiety occupies the allosteric pocket and prevents allosteric activation by progesterone, yet does not activate the enzyme. If CYP3A4 conformational dynamics, as measured by HDX-MS, are indeed reporting on allosteric mechanisms, the G481C-PGM bioconjugate is expected to have a similar HDX profile as the allostery-mimicking systems for structural elements involved in binding the allosteric effector, but not for those elements implicated in activity enhancement. In contrast, the agonistic system is activated even though the PGM label does not occupy the progesterone allosteric pocket (this bioconjugate is further activated by progesterone). We therefore anticipate the HDX profile of L482C-PGM to be comparable to that of the allostery-mimicking systems for structural elements implicated in activity improvement, but not for those elements associated with effector binding. Comparison between the antagonistic (G481C) and the allostery-mimicking (F108C and F215C) enzymes may help us confirm the location of the allosteric site (from the HDX uptake patterns they share) and to identify structural dynamics changes specific to allosteric activation (by identifying where their HDX uptake patterns differ). Our data show that the regions most affected by bioconjugation of CYP3A4 G481C (the C-, F-, F'-, H- helices and the K/β1-loop) all become more rigid after PGM bioconjugation (Figure 2B, S6, S10). Similar to the allostery-mimicking enzymes, rigidification of the F'-helix (peptide 221-226) is observed for the antagonistic system, consistent with PGM occupying the same putative allosteric site, but likely in an orientation that does not trigger activation. Interestingly, the F-helix (peptide 193-213), which experienced a drastic increase in flexibility in the allostery-mimicking bioconjugates, undergoes a significant rigidification in the antagonist bioconjugate. This further supports our earlier proposal that flexibility in the F-helix is linked to allosteric activation of CYP3A4. In contrast to the allostery-mimicking and antagonistic systems, no rigidification is observed around the allosteric pocket (e.g. F'-helix) upon PGM conjugation to the agonistic system (L482C) consistent with the PGM-label being oriented outside of the   allosteric pocket. The regions of the L482C protein most affected by PGM bioconjugation all increase in flexibility (Figure 2C, S6, S11), including the C- and the F-helices (peptides 123-137, 189-212) that also become more flexible in the allostery-mimicking enzymes. Thus, our HDX-MS data with the agonistic system further suggests that flexibility in these regions may be important to allosteric activation of the enzyme.
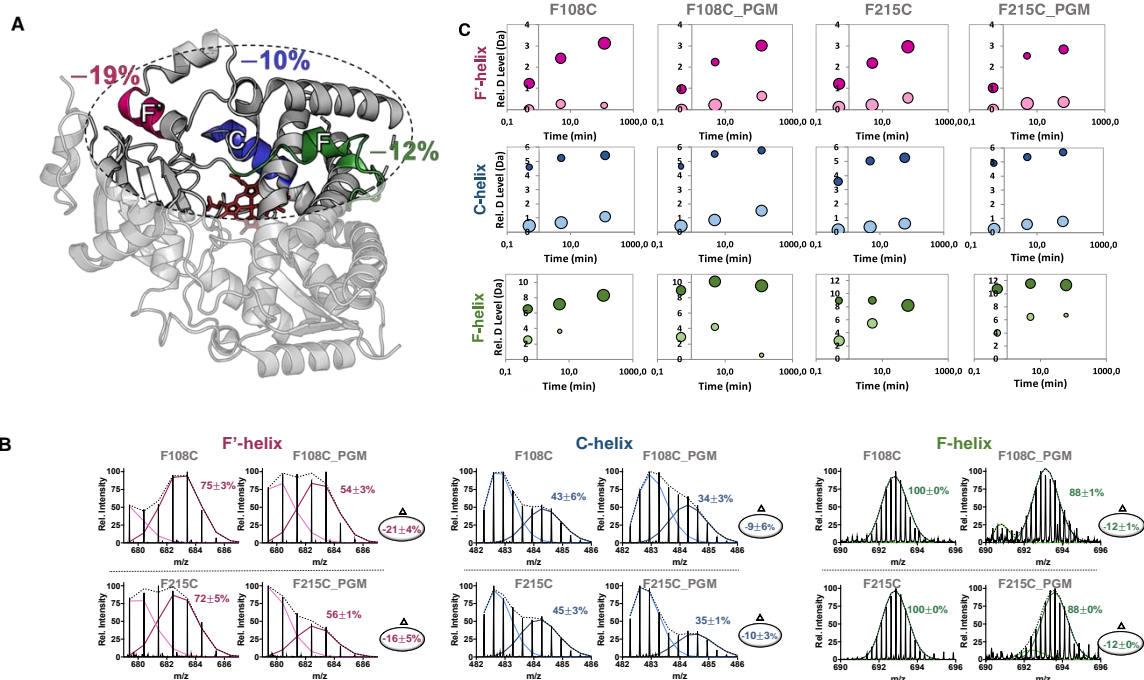
Figure 3. Bimodal exchange profiles of unconjugated and PGM-conjugated allostery-mimicking mutants for three regions relevant to allosteric activation. (**A**) The C- (blue), F- (green) and F'-(pink) helices are highlighted on the CYP3A4 structure (PDB: 1W0F). The percentages quantifiy the decrease in the relative abundance of the highly-exchanged species for these regions after PGM bioconjugation in the two allostery mimics (F108C, F215C). (**B**) The bimodal isotope distributions for peptides derived from the F'-, C- and F-helices are colored to match the CYP3A4 structure in (**A**). The more highly-exchanged population is shown in the darker shade. The spectra were acquired after 120 min (F108C) or 60 min (F215C) of continuous deuterium exchange. Additional deuteration time points for F108C and F215C and their PGM conjugates can be found in Figure S16 and S17, respectively. The relative abundance of the highly-exchanged population is indicated in each panel, and the relative abundance difference between the PGM-conjugate and the unconjugated mutant is shown in the circle next to each state comparison. In both enzymes, PGM conjugation favors the poorly-exchanged conformation (**C**) Bubble plots showing the deuterium uptake (Da) over time for the peptides in (**B**). The size of the bubbles denotes the relative proportions of the unexchanged (paler shades) and highly-exchanged (darker shades) populations. Note that both the poorly- and highly-exchanged conformnations continue to uptake deuterium over time, suggesting a combination of both EX1 and EX2 exchange kinetics (i.e. the mixed EXX kinetics regime). See text for additional details.

Bimodal deuterium exchange profiles reveal the involvement of conformational selection in allostery

Under native conditions, most proteins uptake deuterium in the EX2 regime, where the protein samples unfolded conformations that rapidly re-fold at rates much greater than the rate of deuterium chemical exchange.[23] EX2 kinetics result in a gradual shift of the peptide isotope distribution over time. This exchange pattern was observed for most of the peptides identified in our analysis (Figure S15). However, careful inspection of the mass spectra allowed us to identify peptides that exhibit a bimodal isotope distribution pattern. This exchange behavior (the EX1 regime) is observed when structural elements sample open conformations that re-fold at rates slower than the rate of deuterium chemical exchange, and could indicate the formation of long-lived conformational states. Strikingly, the peptides with such a bimodal isotope distribution were mainly restricted to regions of CYP3A4 involved in allosteric activation (the C-, F- and F'-helices) (Figure 3A). The bimodal isotope patterns were deconvoluted using HX-express software[31] in order to quantify the fractional abundances of the relatively poorly-exchanged and highly-exchanged peptide populations as a function of exchange time (Figure 3B, and S16-S19). Importantly, the impact of PGM-conjugation on the peptide isotope distributions was found to differ between the bioconjugates, which could imply that specific conformational changes are associated with effector binding. For the allostery-mimicking enzymes (F108C and F215C), PGM conjugation stabilized the poorly-exchanged population from the C-, F-, and F' helices (Figure 3B, S16, S17). In contrast, PGM conjugation to the antagonistic (G481C) or agonistic (L482C) enzymes had either no impact on the bimodal isotope distribution of these peptides, or favored the more highly-exchanged population (Figure S18, S19). Cumulatively, these data suggest that binding of the PGM ligand to the allosteric pocket in F108C and F215C is changing the equilibrium between the poorly-exchanged and highly-exchanged conformations of the C-, F-, and F'-helices. Despite the fact that PGM stabilizes a more slowly exchanging form of the C- and the F-helices in the allostery mimics, both the poorly- and highly-exchanged populations of C-, F-, and F-helix peptides uptake additional deuterium over time (Figure 3C). This suggests the presence of additional conformational dynamics in these helices (occurring in the EX2 regime) that expose other exchange sites in the protein backbone. Thus, this mixed EX1 and EX2 behavior (denoted as EXX) reveals distinct effects of PGM bioconjugation, resulting in an overall increase in flexibility for the C- and F-helices (increased deuterium uptake), while favoring a relatively poorly or slowly exchanging conformation.

Bioconjugation is a valuable tool to capture allosteric structural changes

At concentrations below 25 μM, progesterone positively modulates the activity of CYP3A4 towards several substrates (*e.g.* BFC, carbamazepine, nevirapine).[22,32,33] Above this concentration, progesterone competes with the substrate for oxidation.[22,34] Therefore, one would expect the

differential HDX profile of unlabeled CYP3A4 F215C (known to be activated by progesterone) in the presence and absence of progesterone (20 μM) to resemble the differential HDX profile of the allostery-mimicking F215C-PGM bioconjugate. However, binding of free progesterone to the F215C enzyme resulted in a significantly different H/D uptake profile (Figure 4, Figure S7, S12). Namely, peptides derived from the A/A'-, the G- and the I-helices show an increase in flexibility, which represent changes that were not observed in the allostery mimics (Figure 2A). Interestingly, the F-, F-', and G'-helices did not undergo significant changes in deuterium uptake in the presence of 20 μM progesterone, clearly suggesting a distinct binding mode relative to the covalently tethered PGM under our conditions. In the absence of another substrate for oxidation (*e.g.* BFC), it appears that progesterone may not have a long residence time in the allosteric pocket, and may instead relocate to the active site (Figure 4B). Progesterone binding in the active site could also explain the change in dynamics observed in the active site portion of the I-helix. These data imply that the structural dynamics changes triggered by progesterone binding to the allosteric site differ from those associated with binding in the active site. Importantly, these results highlight the utility of the bioconjugation approach, which proved necessary to reveal the structural perturbations specifically associated with allosteric activation.
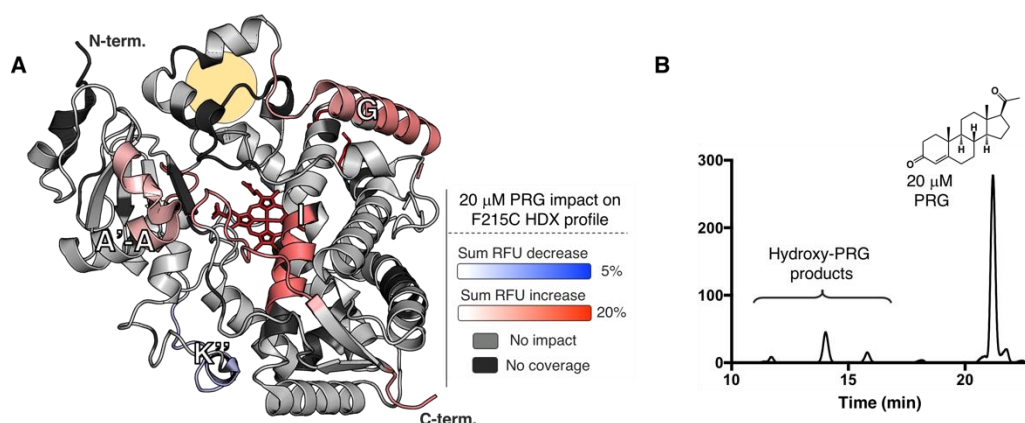

Figure 4. Common features of the differential HDX profiles of the CYP3A4 F215C mutant in the presence of 20 μM progesterone (PRG). (**A**) Regions highlighted in blue become more rigid in the presence of progesterone, while regions in red become more flexible. A yellow circle designates the position of the putative allosteric site of CYP3A4. (**B**) HPLC-based activity assay of the CYP3A4 F215C mutant in the presence of 20 μM progesterone, a concentration at which progesterone behaves as a positive effector in the presence of other substrates. The elution of hydroxylated progesterone products between 12-16 min indicates that progesterone is also binding to the active site and serving as a substrate under these conditions. The complete list of peptides that underwent significant H/D exchange upon PGM conjugation is provided in Figures S6 (F108C) and S7 (F215C).

Discussion

We have developed a set of functionally distinct CYP3A4-PGM bioconjugates that exhibit a range of kinetic behaviors.[22] For the CYP3A4 F108C and F215C mutants, PGM bioconjugation mimics allostery by increasing enzyme activity and preventing further activation by free progesterone, consistent with PGM occupying the allosteric site. In contrast, PGM bioconjugation to the CYP3A4 G481C mutant led to an antagonistic behavior, where PGM occupies the allosteric site (prevents progesterone from activating the enzyme), but does not activate the enzyme itself. Finally, bioconjugation of PGM to the CYP3A4 L482C variant resulted in a system with agonistic behavior, where the enzyme was activated by PGM bioconjugation, but the allosteric site remained available for progesterone activation. Together, these bioconjugates provide a unique toolbox to study the underlying mechanisms of allostery in CYP3A4. Herein, we demonstrate the utility of combining bioconjugation and HDX-MS to characterize allosteric mechanisms. The results

presented advance our mechanistic understanding of CYP3A4 in several ways: i) they confirm the existence of functionally relevant flexible regions; ii) confirm that the F'-helix of CYP3A4 is part of the allosteric site; iii) identify structural elements involved in CYP3A4 allosteric activation, notably the conformational flexibility of the F-helix; and iv) reveal the involvement of conformer selection in allostery.

To determine the impact of PGM bioconjugation on the structural dynamics of CYP3A4, HDX-MS profiles of both unconjugated and PGM-conjugated mutants were compared. Different regions of the protein partially gained or lost their ability to uptake deuterium upon bioconjugation, suggesting that PGM triggers changes in CYP3A4 structural dynamics. Some of these dynamic perturbations may reflect structural changes involved in allostery, while others may result from the covalent modification itself. Therefore, not all deuterium uptake changes observed upon bioconjugation are necessarily relevant to allostery or are strictly associated with ligand binding. Focusing on the similarities in the deuterium uptake differences of two different allostery-mimicking bioconjugates (F108C and F215C) enabled us to assign dynamic changes induced specifically by PGM binding to the allosteric site (Figure 2A). These regions include the C- and F-helices, and H/I-loop (which become more flexible), and the E-, F'- G'-, and K-helices (which become more rigid). Some of these elements are within the most highly dynamic regions of CYP3A4 (Figure S3), suggesting that their flexibility may be required to sample allosterically-activated enzyme conformations.

We also compared the deuterium uptake profiles of these allostery mimics with CYP3A4-PGM conjugates that exhibit antagonistic and agonistic behavior. The antagonistic bioconjugate exhibited similar RFU changes in the F', H- and K-helices upon PGM conjugation. Thus, these HDX perturbations may reflect effects of PGM binding on the enzyme, rather than an allosteric process that results in enzyme activation. On the other hand, comparison of the agonistic bioconjugate with the allostery-mimicking systems enabled us to identify linked elements (the C-, F-, G' and H-helices) with shared H/D uptake patterns that may report directly on allosteric enzyme activation (Figure 2C). In particular, the largest change in deuterium uptake in the allostery-mimicking bioconjugates occurs in the F-helix, a region which shows highly variable conformations between the different crystal structures of CYP3A4 (Figure S23B-C). Upon PGM bioconjugation, the F-helix becomes more flexible in the allostery mimics and agonistic system (Figure 2A, C) but not in the antagonistic system (Figure 2B). These data suggest that flexibility in the F-helix is likely correlated specifically with allosteric activation. We propose that reorganization of the F-helix may involve a lost interaction between Arg212 and residues of the I-helix, and reorientation of Arg212 away from the active site. This movement may facilitate proton transfer by the adjacent Thr309 residue of the I-helix, essential to oxygen activation by the heme, and may modulate the shape and size of the active site.[29,35–38] In addition to the F-helix, the C-helix also becomes more dynamic in all of the activated bioconjugates, but not in the antagonist system. Noticeably, the C-helix is located below the entrance of the putative product egress channel 2e (Figure S22) and is also involved in binding to the P450 reductase redox partner. Its conformational flexibility may thus play a role in the trafficking of small molecules and/or in the interaction of CYP3A4 with the cytochrome P450 reductase.[39,40] Another structural dynamics change observed was the rigidification of the active site K/β1-loop in the allostery-mimicking and antagonist bioconjugates, but not in the agonist conjugate. Located near the heme prosthetic group, the K/β1-loop is expected to participate in productive substrate binding during catalysis (Figure 22).[41]

Important insights into the location of the CYP3A4 allosteric site came from a crystal structure in which the substrate progesterone was found to bind at a site distal to the heme, near the F'-helix (Figure S23A).[29] Although it has been speculated that this peripheral binding pocket may stem from a crystallographic artifact, many biochemical and biophysical studies support the hypothesis that the F'-helix is involved in effector binding and allosteric activation.[18,30,32,42–49] How ligand binding in this region may lead to CYP3A4 catalytic enhancement remains unknown. Structural changes leading to allosteric activation can be dynamic and transient, making them difficult to fully capture with X-ray crystallography. Indeed, comparing the structures of the substrate-free CYP3A4 (PDB: 1W0E, 1TQN)[29,50] to the progesterone-bound complex (PDB: 1W0F, 5A1P),[29,51] reveals no drastic reorganization, even though the biochemical evidence for allosteric activation is strong. Differential HDX profiles for the allostery-mimicking and antagonist systems

revealed a rigidification of the F'-helix, consistent with binding of the covalently-tethered PGM label to the allosteric site deduced originally from X-ray crystal structures.[29] Further reinforcing this proposition, the organization of the F'-helix was not observed for the agonistic system, consistent with the available progesterone binding site in this conjugate.[22] Thus, these modified enzymes enabled us to distinguish structural effects relevant to allosteric enzyme activation from those that reflect ligand binding or covalent modification itself. The covalent attachment of PGM also proved essential to prevent relocalization of the effector ligand from the allosteric site to the active site (Figure 4). Indeed, we were unable to observe structural organization of the F'-helix in the presence of free progesterone (Figure 4). We attribute this lack of an HDX perturbation to weak binding of progesterone to the allosteric site in the absence of a substrate for oxidation – a finding that validates the effectiveness of our covalent conjugation strategy to reveal allosteric mechanisms.

Lastly, analysis of the bimodal isotope patterns observed for some peptides in our study suggests that PGM conjugation in the allostery mimics stabilizes a well-structured conformation of the C-, F- and F'-helices (Figure 3). In contrast, with the antagonist and agonist systems the effect of PGM conjugation on the EX1 kinetics was not significant for the F- and F'- helices, and favored the more highly-exchanged population in the C-helix (Figure S18, S19). Thus, the EX1 structural dynamics of the allosterically-activated F108C-PGM and F215C-PGM enzymes are distinct from the other bioconjugates. Our data support a model where PGM binding near the F'-helix triggers an allosteric effect that favors a more structured, slowly-exchanging sub-population of the C-helix (involved in reductase binding and electron transfer) and the F-helix (involved in active site access and catalysis). Interestingly, the channel-gating B'-helical region (for which the deuterium uptake was not affected by PGM conjugation of the allostery mimics), also exhibited EX1 behavior in all of the CYP3A4 variants. Paço *et al.* have recently reported EX1 behavior in the B'-helix of P450 aromatase, noting that the bimodal isotope distribution was abolished in the presence of the substrate.[52] The observation of EX1 kinetics in the B'-helix of different CYPs could suggest the existence of a conserved dynamic feature that is sensitive to ligand binding. Moving forward, it will be interesting to examine the extent to which the conformational dynamics revealed in the present study are shared by other CYPs. This information could help to better assess and predict the roles of allostery in modulating CYP function.

Conclusion

In summary, we have demonstrated that combining bioconjugation and HDX-MS is a powerful strategy to study the underlying structural dynamics of allostery. This unique approach allowed us to overcome issues related to weak substrate binding, ligand relocalization, and the discrimination between dynamic changes caused by binding from those involved in activity enhancement. The method proved useful not only to confirm the location of the previously suggested CYP3A4 allosteric site, but also to identify a series of structural elements (*e.g.* the K/β1-loop and F-helix) specifically involved in activity enhancement. Allosteric activation or inhibition of CYP3A4 by small molecule pharmaceuticals (*e.g.* midazolam and warfarin) is an important mechanism associated with drug interactions in humans.[9,53,54] Such adverse interactions are currently established empirically, but a better mechanistic understanding of the phenomena may improve *in silico* predictions, thereby facilitating the rational design of pharmaceuticals with lower potential for adverse drug interactions. Considering that allostery is ubiquitous in biological systems, the general approach outlined in this work should find broader application in unraveling the allosteric properties of other enzyme systems.

Acknowledgements

Supporting Information: Experimental methods, HDX experimental conditions, detailed differential HDX uptake data and bimodal mass distribution spectra, and other CYP3A4 structural informative figures are supplied as supporting information

References

(1)   Perutz, M. F. Mechanisms of cooperativity and allosteric regulation in proteins. *Q. Rev. Biophys.* **1989**, *22* (2), 139–236.

(2)   Monod, J.; Wyman, J.; Changeux, J. P. On the nature of allosteric transitions: A plausible model. *J. Mol. Biol.* **1965**, *12* (1), 88–118.

(3)   Sheean et al., 2013. Allostery: an illustrated definition for the 'second secret of life'. *Trends Biochem. Sci.* **2008**, *33* (9), 420–425.

(4)   Dedecker, B. S. Allosteric drugs: Thinking outside the active-site box. *Chem. Biol.* **2000**, *7* (5), 103–107.

(5)   Koshland, D. E.; Nemethy, J. G.; Filmer, D. Comparison of Experimental Binding Data and Theoretical Models in Proteins Containing Subunits. *Biochemistry* **1966**, *5* (1), 365–385.

(6)   Ribeiro, A. A. S. T.; Ortiz, V. A Chemical Perspective on Allostery. *Chem. Rev.* **2016**, *116* (11), 6488–6502.

(7)   Dokholyan, N. V. Controlling Allosteric Networks in Proteins. *Chem. Rev.* **2016**, *116* (11[1] N. V. Dokholyan, Chem. Rev. 2016, 116, 6463–6487.), 6463–6487.

(8)   Hlavica, P.; Lewis, D. F. V. V. Allosteric phenomena in cytochrome P450-catalyzed monooxygenations. *Eur. J. Biochem.* **2001**, *268* (18), 4817–4832.

(9)   Sligar, S. G.; Denisov, I. G. Understanding Cooperativity in Human P450 Mediated Drug-Drug Interactions. *Drug Metab. Rev.* **2007**, *39* (2–3), 567–579.

(10)   Davydov, D. R.; Halpert, J. R. Allosteric P450 Mechanisms: Multiple Binding Sites, Multiple Conformers or Both? *Expert Opin. Drug Metab. Toxicol.* **2008**, *4* (12), 1523–1535.

(11)   Guengerich, F. P. Cytochrome P450 and Chemical Toxicology. *Chem. Res. Toxicol.* **2008**, *21* (Table 1), 70–83.

(12)   Denisov, I. G.; Baas, B. J.; Grinkova, Y. V.; Sligar, S. G. Cooperativity in Cytochrome P450 3A4: Linkages in Substrate Binding, Spin State, Uncoupling, and Product Formation. *J. Biol. Chem.* **2007**, *282* (10), 7066–7076.

(13)   Korzekwa, K. R.; Krishnamachary, N.; Shou, M.; Ogai, A.; Parise, R. A.; Rettie, A. E.; Gonzalez, F. J.; Tracy, T. S. Evaluation of atypical cytochrome P450 kinetics with two-substrate models: evidence that multiple substrates can simultaneously bind to cytochrome P450 active sites. *Biochemistry* **1998**, *37* (12), 4137–4147.

(14)   Davydov, D. R.; Davydova, N. Y.; Sineva, E. V; Kufareva, I.; Halpert, J. R. Pivotal role of P450-P450 interactions in CYP3A4 allostery: The case of a-naphthoflavone. *Biochem. J.* **2013**, *453* (2), 219–230.

(15)   Lampe, J. N.; Fernandez, C.; Nath, A.; Atkins, W. M. Articles Nile Red Is a Fluorescent Allosteric Substrate of Cytochrome P450 3A4 †. *Biochemistry* **2008**, *47* (1), 509–516.

(16)   Denisov, I. G.; Sligar, S. G. A novel type of allosteric regulation: functional cooperativity in monomeric proteins. *Arch. Biochem. Biophys.* **2012**, *519* (2), 91–102.

(17)   Atkins, W. M.; Wang, R. W.; Lu, A. Y. H. H. Allosteric behavior in cytochrome P450-dependent in vitro drug-drug interactions: A prospective based on conformational dynamics. *Chem. Res. Toxicol.* **2001**, *14* (4), 338–347.

(18)   Harlow, G. H.; Halpert, J. R. Alanine-scanning Mutagenesis of a Putative Substrate Recognition Site in Human Cytochrome P450 3A4. *J. Biol. Chem.* **1997**, *272* (9), 5396–5402.

(19)   Hosea, N. A.; Miller, G. P.; Guengerich, F. P. Elucidation of distinct ligand binding sites for cytochrome P450 3A4. *Biochemistry* **2000**, *39* (6), 5929–5939.

(20)   Konermann, L.; Pan, J.; Liu, Y. H. Hydrogen exchange mass spectrometry for studying protein structure and dynamics. *Chem. Soc. Rev.* **2011**, *40* (3), 1224–1234.

(21)   Polic, V.; Auclair, K. Allosteric Activation of Cytochrome P450 3A4 via Progesterone Bioconjugation. *Bioconjug. Chem.* **2017**, *28* (4), 885–889.

(22)   Ducharme, J.; Polic, V.; Auclair, K. A Covalently Attached Progesterone Molecule Outcompetes the Binding of

Free Progesterone at an Allosteric Site of Cytochrome P450 3A4. *Bioconjug. Chem.* **2019**, *30* (6), 1629–1635.

(23)   Ferraro, D. M.; Robertson, A. D. EX1 Hydrogen Exchange and Protein Folding. *Biochemistry* **2004**, *43* (3), 587–594.

(24)   Ekroos, M.; Sjogren, T. Structural Basis for Ligand Promiscuity in Cytochrome P450 3A4. *Proc. Natl. Acad. Sci.* **2006**, *103* (37), 13682–13687.

(25)   Treuheit, N. A.; Redhair, M.; Kwon, H.; McClary, W. D.; Guttman, M.; Sumida, J. P.; Atkins, W. M. Membrane Interactions, Ligand-Dependent Dynamics, and Stability of Cytochrome P4503A4 in Lipid Nanodiscs. *Biochemistry* **2016**, *55* (7), 1058–1069.

(26)   Chuo, S.-W. W.; Liou, S. H.; Wang, L. P.; Britt, R. D.; Poulos, T. L.; Sevrioukova, I. F.; Goodin, D. B. Conformational Response of N-Terminally Truncated Cytochrome P450 3A4 to Ligand Binding in Solution. *Biochemistry* **2019**, *58* (37), 3903–3910.

(27)   Baas, B. J.; Denisov, I. G.; Sligar, S. G. Homotropic cooperativity of monomeric cytochrome P450 3A4 in a nanoscale native bilayer environment. **2004**, *430*, 218–228.

(28)   Lau, A. M. C.; Ahdash, Z.; Martens, C.; Politis, A. Deuteros: Software for Rapid Analysis and Visualization of Data from Differential Hydrogen Deuterium Exchange-Mass Spectrometry. *Bioinformatics* **2019**, *35* (17), 3171–3173.

(29)   Williams, P. A.; Cosme, J.; Vinkovic, D. M.; Alison, W.; Angove, H. C.; Day, P. J.; Clemens, V.; J.T, I.; Jhoti, H. Crystal Structures of Human Cytochrome P450 3A4 Bound to Metyrapone and Progesterone. *Science (80-.).* **2004**, *305* (5684), 683–686.

(30)   Davydov, D. R.; Rumfeldt, J. A. O.; Sineva, E. V.; Fernando, H.; Davydova, N. Y.; Halpert, J. R. Peripheral Ligand-Binding Site in Cytochrome P450 3A4 Located with Fluorescence Resonance Energy Transfer (FRET). *J. Biol. Chem.* **2012**, *287* (9), 6797–6809.

(31)   Guttman, M.; Weis, D. D.; Engen, J. R.; Lee, K. K. Analysis of overlapped and noisy hydrogen/deuterium exchange mass spectra. *J. Am. Soc. Mass Spectrom.* **2013**, *24* (12), 1906–1912.

(32)   Denisov, I. G. Grinkova, Y. V., Nandigrami, P., Shekhar, M. S., Tajkhorshid, E., Sligar, S. G. Allosteric Interactions in Human Cytochrome P450 CYP3A4: The Role of Phenylalanine 213. *Biochemistry* **2019**, *58* (10), 1411–1422.

(33)   Nakamura, H.; Nakasa, H.; Ishii, I.; Ariyoshi, N.; Igarashi, T.; Ohmori, S.; Kitada, M. Effects of Endogenous Steroids on CYP3A4-Mediated Drug Metabolism by Human Liver Microsomes. *Drug Metab. Dispos.* **2002**, *30* (5), 534–540.

(34)   Domanski, T. L.; He, Y.-A. A.; Khan, K. K.; Roussel, F.; Wang, Q.; Halpert, J. R. Phenylalanine and tryptophan scanning mutagenesis of CYP3A4 substrate recognition site residues and effect on substrate oxidation and cooperativity. *Biochemistry* **2001**, *40* (34), 10150–10160.

(35)   Sevrioukova, I. F.; Poulos, T. L. Structural and Mechanistic Insights into The Interaction of Cytochrome P4503A4 with Bromoergocryptine, a Type I Ligand. *J. Biol. Chem.* **2012**, *287* (5), 3510–3517.

(36)   Sevrioukova, I. F. High-Level Production and Properties of the Cysteine-Depleted Cytochrome P450 3A4. *Biochemistry* **2017**, *56* (24), 3058–3067.

(37)   Guo, Z.; Sevrioukova, I. F.; Denisov, I. G.; Zhang, X.; Chiu, T. L.; Thomas, D. G.; Hanse, E. A.; Cuellar, R. A. D.; Grinkova, Y. V.; Langenfeld, V. W.; Swedien, D. S.; Stamschror, J. D.; Alvarez, J.; Luna, F.; Galván, A.; Bae, Y. K.; Wulfkuhle, J. D.; Gallagher, R. I.; Petricoin, E. F.; Norris, B.; Flory, C. M.; Schumacher, R. J.; O'Sullivan, M. G.; Cao, Q.; Chu, H.; Lipscomb, J. D.; Atkins, W. M.; Gupta, K.; Kelekar, A.; Blair, I. A.; Capdevila, J. H.; Falck, J. R.; Sligar, S. G.; Poulos, T. L.; Georg, G. I.; Ambrose, E.; Potter, D. A. Heme Binding Biguanides Target Cytochrome P450-Dependent Cancer Cell Mitochondria. *Cell Chem. Biol.* **2017**, *24* (10), 1259–1275.

(38)   Sevrioukova, I. Interaction of Human Drug-Metabolizing CYP3A4 with Small Inhibitory Molecules. *Biochemistry* **2019**, *58*, 930–939.

(39)   Cojocaru, V.; Winn, P. J.; Wade, R. C. The Ins and Outs of Cytochrome P450s. *Biochim. Biophys. Acta - Gen. Subj.* **2007**, *1770* (3), 390–401.

(40)   Ortiz de Montellano, P. R. *Cytochrome P450: Structure, Mechanism, and Biochemistry*, 4th red.; Ortiz de Montellano, P. R., Red.; Springer International Publishing, 2015.

(41)   Müller, C. S.; Knehans, T.; Davydov, D. R.; Bounds, P. L.; Von Mandach, U.; Halpert, J. R.; Caflisch, A.; Koppenol, W. H. Concurrent Cooperativity and Substrate Inhibition in the Epoxidation of Carbamazepine by Cytochrome P450 3A4 Active Site Mutants Inspired by Molecular Dynamics Simulations. *Biochemistry* **2015**, *54*

(3), 711–721.

(42) Denisov, I. G.; Mak, P. J.; Grinkova, Y. V.; Bastien, D.; Bérubé, G.; Sligar, S. G.; Kincaid, J. R. The Use of Isomeric Testosterone Dimers to Explore Allosteric Effects in Substrate Binding to Cytochrome P450 CYP3A4. *J. Inorg. Biochem.* **2016**, *158*, 77–85.

(43) Marsch, G. A.; Carlson, B. T.; Guengerich, F. P. 7,8-Benzoflavone Binding to Human Cytochrome P450 3A4 Reveals Complex Fluorescence Quenching, Suggesting Binding at Multiple Protein Sites. *J. Biomol. Struct. Dyn.* **2018**, *36* (4), 841–860.

(44) Roberts, A. G.; Atkins, W. M. Energetics of Heterotropic Cooperativity Between a-Naphthoflavone and Testosterone Binding to CYP3A4. *Arch. Biochem. Biophys.* **2007**, *463* (1), 89–101.

(45) Sineva, E. V.; Rumfeldt, J. A. O.; Halpert, J. R.; Davydov, D. R. A Large-Scale Allosteric Transition in Cytochrome P450 3A4 Revealed by Luminescence Resonance Energy Transfer (LRET). *PLoS One* **2013**, *8* (12), e83898.

(46) Ichikawa, T.; Tsujino, H.; Miki, T.; Kobayashi, M.; Matsubara, C.; Miyata, S.; Yamashita, T.; Takeshita, K.; Yonezawa, Y.; Uno, T. Allosteric Activation of Cytochrome P450 3A4 by Efavirenz Facilitates Midazolam Binding. *Xenobiotica* **2018**, *48* (12), 1227–1236.

(47) Harlow, G. R.; Halpert, J. R. Analysis of Human Cytochrome P450 3A4 Cooperativity: Construction and Characterization of a Site-Directed Mutant that Displays Hyperbolic Steroid Hydroxylation Kinetics. *Proc. Natl. Acad. Sci. U. S. A.* **1998**, *95* (12), 6636–6641.

(48) Redhair, M.; Hackett, J. C.; Pelletier, R. D.; Atkins, W. M. Dynamics and Location of the Allosteric Midazolam Site in Cytochrome P4503A4 in Lipid Nanodiscs. *Biochemistry* **2020**, *59*, 766–779.

(49) Denisov, I. G.; Baylon, J. L.; Grinkova, Y. V.; Tajkhorshid, E.; Sligar, S. G. Drug-Drug Interactions between Atorvastatin and Dronedarone Mediated by Monomeric CYP3A4. *Biochemistry* **2018**, *57* (5), 805–816.

(50) Yano, J. K.; Wester, M. R.; Schoch, G. A.; Griffin, K. J.; Stout, C. D.; Johnson, E. F. The Structure of Human Microsomal Cytochrome P450 3A4 Determined by X-Ray Crystallography to 2.05-Å Resolution. *J. Biol. Chem.* **2004**, *279* (37), 38091–38094.

(51) Sevrioukova, I. F.; Poulos, T. L. Anion-Dependent Stimulation of CYP3A4 Monooxygenase. *Biochemistry* **2015**, *54* (26), 4083–4096.

(52) Paco, L.; Zarate-Perez, F.; Clouser, A. F.; Atkins, W. M.; Hackett, J. C. Dynamics and mechanism of androstenedione binding to membrane-associated aromatase. *Biochemistry* **2020**, *59* (33), 2999–3009.

(53) E, A. R.; Wang, R. W.; Newton, D. J.; Liu, N.; Atkins, W. M.; Lu, A. Y. H. Human Cytochrome P-450 3a4 : in Vitro Drug-Drug Interaction Patterns. *Pharmacology* **2000**, *28* (3), 360–366.

(54) Maxa, C. C. O. and J. L. Drug interactions due to cytochrome P450. *Proc. (Bayl. Univ. Med. Cent).* **2000**, *13* (4), 421–423.